

## RESEARCH ARTICLE

# Fuzzy Extended State Observer for Robust Sliding Mode Control of Piezoelectric Actuators

MARYAM NAGHDI AND IMAN IZADI 

Department of Electrical and Computer Engineering, Isfahan University of Technology, Isfahan 8415683111, Iran

Corresponding author: Iman Izadi (iman.izadi@iut.ac.ir)

**ABSTRACT** Piezoelectric actuators are widely used in micro and nano-positioning systems for accurate movement. However, they exhibit some nonlinearities, particularly hysteresis, which makes precise control rather challenging. Many methods are available in the literature to compensate for the hysteresis effect in piezoelectric actuators, but often a model of the actuator is required for this purpose. Identification of such a model is challenging too. In this paper, we propose using a robust observer-based controller for precise motion tracking of piezoelectric actuators without the need for a hysteresis model. The controller consists of a fuzzy extended state observer (FESO) to estimate the hysteresis and other nonlinearities, as well as model uncertainties and external disturbances. Subsequently, a robust sliding-mode controller is designed and added to the framework. Joint stability analysis guarantees the stability and tracking performance of the proposed combined controller. Simulation and experimental results confirm the performance of the proposed controller compared to some other techniques.

**INDEX TERMS** Precision motion control, piezoelectric actuator, hysteresis, fuzzy extended state observer, sliding mode control.

## I. INTRODUCTION

Precision motion control is an important research subject in the field of micro and nano positioning. Smart material actuators are suitable tools used to provide precision motion control [1]. Piezoelectric actuators (PEA), with high resolution, swift response, and high stiffness, are the most renowned ones [2]. PEAs have been used in different applications, such as cell puncture mechanisms [3], surgical devices (a ventilation tube applicator) [4], scanning probe microscopy (SPM) [5], adaptive optics, aviation, micromanipulator [6], and high-precision machine tools [7]. However, the performance of PEAs is limited by their intrinsic nonlinear dynamics, particularly hysteresis [7], [8]. Hysteresis can cause a dissimilarity between the control system output and the desired position [8]; additionally, it can be the reason for system instability [8], [9] and output oscillation [9], [10]. To obtain precise motion tracking of the PEA, the design of an effective compensator is, therefore, necessary.

The associate editor coordinating the review of this manuscript and approving it for publication was Feiqi Deng .

Different models, based on various concepts, have been proposed over the years to describe the behavior of PEAs, including their hysteresis. The Bouc-Wen model [11], the Duhem model [12], the Maxwell-Slip model [13], the Prandtl-Ishlinskii model [14], and the Preisach model [8] are some of the well-known models used for hysteresis modeling in the literature.

One of the traditional techniques of hysteresis compensation is open-loop control, also known as the feed-forward compensator [10]. In this technique, the compensator is an inverse hysteresis model cascaded with the PEA. Generally, the open-loop structure has the well-known drawback that it cannot compensate for modeling errors, uncertainties, and external disturbances [3], [10]. Additionally, open-loop hysteresis compensation requires an accurate hysteresis model [3]. Moreover, it is not always possible to obtain an inverse of the model. To enhance the performance of open-loop controllers, some researchers have suggested feedback control along with the inversion-free feed-forward compensator [1], [10], [15].

To compensate for external disturbances and model mismatch, as every control engineer is well aware, closed-loop

control and feedback are required. Many different techniques have been suggested over the years for closed-loop control of PEAs, as reviewed in a number of surveys including [2], [6], and [7]. However, the need for a model for the PEA remains, albeit not as accurate as the case of open-loop control.

To evade the need for a model which requires extra off-line steps of modeling and identification, feedback control algorithms with no hysteresis model were developed. For instance, sliding-mode controller (SMC) with fast reaching law and proportional-integral-differential (PID) sliding surface combined with time delay estimation (TDE) [3]; a combined controller using an extended state observer (ESO) with the SMC and PD controllers for feedback, and radial basis function neural networks for reference generation in feedforward [4]; current-cycle iterative learning control with active disturbance rejection control [16]; and adaptive SMC with uncertainty and disturbance estimation [17] are some of the techniques used for model-free control of PEAs.

Note that neural network models have structural complexities that result in increased computational burden. Adaptive mechanisms can often contribute to increased complexity too [18]. Also, it is impossible to avoid TDE errors since the microcontroller sampling time sets the minimum value for the time delay [19]. Additionally, noisy measurements and nonlinearity of signals along the sampling time cause a time delay error [20].

In this paper, we propose a hysteresis model-free controller with fuzzy extended-state observer (FESO) for PEAs. Due to the fact that the SMC is capable of dealing with different uncertainties and external disturbances [3], [9], we adopt it as the main controller to enhance the tracking performance of PEAs. However, the level of uncertainty and the upper bound for the disturbance directly affects the conservatism of the controller [9]. The control performance, in this case, can be enhanced using a disturbance estimator/observer. Extended state observer (ESO) is a well-known technique used to eliminate the effect of disturbances on the performance of control systems [21]. ESO creates an extra state to estimate internal uncertainty and external disturbances in real time [21] and is often used for active disturbance rejection control [22]. ESO has also been utilized for PEA control [4], [16]. Conventional ESO, however, suffers from a few drawbacks, including chattering in the nonlinear form of ESO [16]; and the peaking value and the convergence rate in the linear form of ESO (LESO) [21], which could negatively impact the control performance.

The objective of the design outlined in this paper is to ensure a satisfactory tracking performance of PEAs for both continuous and discontinuous trajectories in the presence of disturbances and system uncertainties, with high accuracy in both steady and transient performance. Therefore, we propose to employ fuzzy ESO (FESO) [21] to estimate the hysteresis and other disturbances, on top of the robust SMC.

The main contributions of this paper are described as follows:

- The design of the proposed algorithm is based on the second order linear dynamics with unknown hysteresis nonlinearity. Thus, there is no complexity in the basic model and parameters identification of the hysteresis nonlinearity and the calculation of its inverse are not needed.
- The FESO can form a desired transient performance. It can obtain satisfactory estimation without any information about disturbances/uncertainties such as their bounds. Additionally, its fast convergence speed assists in improved control performance.
- The stability analysis of FESO with the controller is studied theoretically based on a joint stability proof. Joint stability refers to the stability of a system in which all components or subsystems operate together. This is important since, the individual stability of subsystems does not guarantee overall stability in nonlinear systems.
- In order to effectively illustrate the crucial role played by estimation tools in enhancing controller performance, we compare a variety of advanced estimation techniques including FESO, LESO, and TDE. By employing these methods, we showcase a deeper understanding of how estimation tools can enhance the performance of controllers in various applications.
- The efficiency of the proposed algorithm is tested for tracking different reference trajectories. The experimental results show that the FESO-SMC controller can ensure a proper trade-off between the convergence rate, peaking value, and tracking accuracy.

## II. PRELIMINARIES

The Bouc-Wen model of PEA, which is used in this paper for observer/controller design is given by [11] as

$$\begin{cases} m\ddot{x}(t) + b\dot{x}(t) + kx(t) = k(du(t) - h(t)) - w(t) \\ \dot{h}(t) = \alpha d\dot{u}(t) - \beta|\dot{u}(t)|h(t) - \gamma\dot{u}(t)|h(t)| \end{cases} \quad (1)$$

where  $u$  is the control signal (driver voltage for PEA), and  $x$  is the system output (position of PEA). Parameters of the linear part are  $m$ ,  $b$ ,  $k$ , and  $d$ , which represent the mass, damping coefficient, stiffness coefficient, and piezoelectric coefficient, respectively. Additionally,  $w(t)$  represents external disturbance, model uncertainty, and other unknown terms. Furthermore,  $h(t)$  is an internal state that accounts for the hysteresis nonlinearity. Parameters of the nonlinear part are:  $\alpha$ ,  $\beta$ , and  $\gamma$ .

Considering  $h(t)$  and  $w(t)$  as uncertainty/disturbance denoted by  $D(t) = -\frac{k}{m}h(t) - \frac{1}{m}w(t)$ , the dynamical model (1) is rewritten as

$$\ddot{x}(t) + \frac{b}{m}\dot{x}(t) + \frac{k}{m}x(t) = \frac{kd}{m}u(t) + D(t) \quad (2)$$

Based on this simplified model, there is no need for hysteresis parameter identification. The uncertainty/disturbance term  $D(t)$  is estimated by the proposed observer, i.e., the fuzzy extended state observer (FESO).

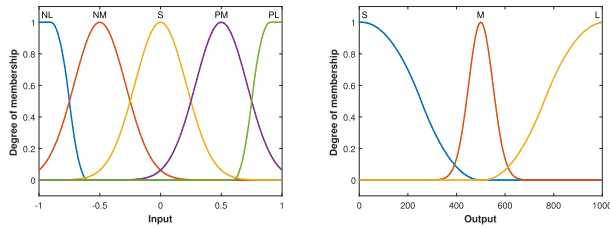


FIGURE 1. Input ( $k_{o1}e_{o1} + k_{o2}\dot{e}_{o1}$ ) (left) and output ( $\omega_o$ ) (right) membership functions of the fuzzy model.

### III. DESIGN OF FESO FOR PEA

Owing to the complexity of the structure of PEAs, as explained before, accurate model extraction is a challenging task [5]. To tackle this challenge, at least partly, the nonlinear (i.e., hysteresis) and disturbance components of the PEA dynamics, represented by  $D(t)$  in (2), are estimated using FESO.

#### A. THE STRUCTURE OF FESO

To design an FESO for the simplified PEA model in (2), the idea is to consider  $D(t)$  as the third state and estimate it [21]. The state-space form of (2) is, therefore, expressed as

$$\begin{cases} \dot{x}_1 = x_2 \\ \dot{x}_2 = -\frac{k}{m}x_1 - \frac{b}{m}x_2 + x_3 + \frac{kd}{m}u \\ \dot{x}_3 = \dot{D} \triangleq \varphi(t) \\ y = x_1 \end{cases} \quad (3)$$

To estimate  $D(t)$  in real-time, FESO is constructed as

$$\begin{cases} \dot{z}_1 = z_2 - \omega_o\beta_1e_{o1} \\ \dot{z}_2 = -\frac{k}{m}z_1 - \frac{b}{m}z_2 + z_3 + \frac{kd}{m}u - \omega_o^2\beta_2e_{o1} \\ \dot{z}_3 = -\omega_o^3\beta_3e_{o1} \\ e_{oi} = z_i - x_i \quad i = 1, 2, 3 \end{cases} \quad (4)$$

and the observer bandwidth  $\omega_o$  is tuned by a fuzzy model with five rules as

- Rule 1: If  $k_{o1}e_{o1} + k_{o2}\dot{e}_{o1}$  is PL then  $\omega_o$  is S
- Rule 2: If  $k_{o1}e_{o1} + k_{o2}\dot{e}_{o1}$  is PM then  $\omega_o$  is M
- Rule 3: If  $k_{o1}e_{o1} + k_{o2}\dot{e}_{o1}$  is S then  $\omega_o$  is L
- Rule 4: If  $k_{o1}e_{o1} + k_{o2}\dot{e}_{o1}$  is NM then  $\omega_o$  is M
- Rule 5: If  $k_{o1}e_{o1} + k_{o2}\dot{e}_{o1}$  is NL then  $\omega_o$  is S

Here  $\beta_i$ ,  $i = 1, 2, 3$  are the tunable parameters of FESO, and  $k_{o1}$  and  $k_{o2}$  are the input scaling factors of the fuzzy model.

The fuzzy system input,  $k_{o1}e_{o1} + k_{o2}\dot{e}_{o1}$ , is fuzzified using linguistic values, positive medium (PM), small (S), and negative medium (NM), which are all represented by Gaussian membership functions; positive large (PL) which is described by an S-shaped membership function; and negative large (NL) which is represented by a Z-shaped membership function, as shown in Fig. 1 (left). Similarly, for the bandwidth  $\omega_o$ , the Gaussian, S-shaped, and Z-shaped membership functions are used for medium (M), large (L),

and small (S), respectively, as shown in Fig. 1 (right). Therefore, the architecture of the fuzzy system consists of minimum implication, singleton fuzzifier, and the center of gravity defuzzifier.

#### B. CONVERGENCE OF FESO

To analyze the convergence of the estimation error, after some mathematical manipulations, the dynamics of FESO observer in (4), is obtained as

$$\dot{e}_o = Ae_o + B'_1e_o - \varphi(t)B_2 \quad (5)$$

where

$$e_o = \begin{bmatrix} e_{o1} \\ e_{o2} \\ e_{o3} \end{bmatrix}, A = \begin{bmatrix} -\omega_o\beta_1 & 1 & 0 \\ -\omega_o^2\beta_2 & 0 & 1 \\ -\omega_o^3\beta_3 & 0 & 0 \end{bmatrix}, B'_1 = \begin{bmatrix} 0 & 0 & 0 \\ -k/m & -b/m & 0 \\ 0 & 0 & 0 \end{bmatrix}, B_2 = \begin{bmatrix} 0 \\ 0 \\ 1 \end{bmatrix}$$

Let  $\varepsilon_i = \frac{e_{oi}}{\omega_o^{i-1}}$ , thus

$$\dot{\varepsilon} = \omega_o A_1 \varepsilon + B_1 \varepsilon - \frac{\varphi}{\omega_o^2} B_2 \quad (6)$$

where

$$\varepsilon = \begin{bmatrix} \varepsilon_1 \\ \varepsilon_2 \\ \varepsilon_3 \end{bmatrix}, A_1 = \begin{bmatrix} -\beta_1 & 1 & 0 \\ -\beta_2 & 0 & 1 \\ -\beta_3 & 0 & 0 \end{bmatrix}, B_1 = \begin{bmatrix} 0 & 0 & 0 \\ -\frac{k}{\omega_o m} & -\frac{b}{m} & 0 \\ 0 & 0 & 0 \end{bmatrix}, B_2 = \begin{bmatrix} 0 \\ 0 \\ 1 \end{bmatrix}$$

Notice the difference between  $B_1$  and  $B'_1$ . Now, if  $\beta_i$ 's are selected properly, then  $A_1$  is Hurwitz. Therefore, the solution of the Lyapunov equation  $A_1^T P + P A_1 = -I$ , i.e.,  $P$  is unique, symmetrical, and positive definite. For the convergence analysis, we assume that  $\varphi$  is bounded, i.e.,  $|\varphi| \leq \delta$ . In the case of the Bouc-Wen model, where  $D(t) = -\frac{k}{m}h(t) - \frac{1}{m}w(t)$ , the assumption requires that rates of change of  $h(t)$  and  $w(t)$  are bounded, which is practically valid. Considering the upper bound

*Theorem 1:* For FESO in (4) and the given fuzzy rules, the observer errors converge to the following regions

$$|e_{oi}| \leq \frac{2\omega_{o\max}^{i-1}\delta\lambda_{\max}(P)}{\omega_{o\min}^2(\omega_{o\min} - 2\|PB_1\|)}, \quad i = 1, 2, 3.$$

*Proof:* A Lyapunov function is selected as  $V_o = \varepsilon^T P \varepsilon$ , where  $P$  is obtained from the Lyapunov equation given above and is positive definite. By using (6), the time derivative of  $V_o$  is obtained as

$$\dot{V}_o = -\omega_o \varepsilon^T \varepsilon + 2\varepsilon^T P B_1 \varepsilon + \frac{2\varepsilon^T P B_1 (-\varphi)}{\omega_o^2} \quad (7)$$

Now, because  $\omega_o$  is tuned by the fuzzy model, it is time-varying, but has lower and upper bounds defined

by  $\omega_{omin} \leq \omega_o \leq \omega_{omax}$ . Then,

$$\dot{V}_o \leq -\omega_{omin}\|\varepsilon\|^2 + 2\|PB_1\|\|\varepsilon\|^2 + \frac{2\delta\lambda_{max}(P)\|\varepsilon\|}{\omega_{omin}^2} \quad (8)$$

Notice that if  $\omega_{omin} > 2\|PB_1\|$  and  $\|\varepsilon\| > \frac{2\delta\lambda_{max}(P)}{\omega_{omin}^2(\omega_{omin}-2\|PB_1\|)}$  then  $\dot{V}_o < 0$ . With the proper choice of fuzzy membership functions and their location,  $\omega_{omin}$  can be selected large enough. Therefore,  $\frac{2\delta\lambda_{max}(P)}{\omega_{omin}^2(\omega_{omin}-2\|PB_1\|)}$  is the upper bound for  $\|\varepsilon\|$ . Thus,  $|e_{oi}| = \omega_o^{i-1}|\varepsilon_i| \leq \omega_{omax}^{i-1}\|\varepsilon\|$ ,  $i = 1, 2, 3$  and the proof is complete.

#### IV. FESO-BASED SLIDING MODE CONTROL OF PEA

To eliminate the undesirable effects of hysteresis and other disturbances on the tracking performance of PEA, FESO is first employed to estimate them; then it is mitigated by the SMC algorithm.

##### A. THE SMC STRUCTURE

In this paper, the control rule of SMC is extracted based on the proportional-derivative (PD) sliding surface. The tracking error is defined as

$$e = x - x_d \quad (9)$$

where  $x$  is the position of PEA and  $x_d$  is the desired position. The PD sliding surface is defined as  $s = \dot{e} + \lambda e$ , where  $\dot{e} = \dot{x} - \dot{x}_d$ , and  $\lambda > 0$  is the design parameter. The time derivative of  $s$  is obtained as

$$\begin{aligned} \dot{s} &= \ddot{x} - \ddot{x}_d + \lambda(\dot{x} - \dot{x}_d) \\ &= -\frac{k}{m}x_1 - \frac{b}{m}x_2 + x_3 + \frac{kd}{m}u - \ddot{x}_d + \lambda(\dot{x} - \dot{x}_d) \end{aligned} \quad (10)$$

Therefore, the control rule is calculated as

$$\begin{aligned} u &= \frac{m}{kd}(\ddot{x}_d + \lambda\dot{x}_d) + \frac{1}{d}x_1 - \frac{m}{kd}z_3 + \left(\frac{b}{kd} - \lambda\frac{m}{kd}\right)z_2 \\ &\quad - k_{c1}s - k_{c2}\operatorname{sgn}(s) \end{aligned} \quad (11)$$

where  $k_{c1}$  and  $k_{c2}$  are the design parameters.

##### B. JOINT STABILITY ANALYSIS OF FESO-SMC CONTROLLER

*Theorem 2:* For system (2) with the state space form (3), the control rule is calculated as (11). With proper selection of the design parameters  $\omega_{omin}$  and  $k_{c2}$ , the convergence of the tracking error (9) to zero is assured.

*Proof:* First notice that in the control rule (11), we explicitly use the first state  $x_1$  (the PEA position) which is measured by accurate sensors. For the other two states  $x_2, x_3$ , their estimation from the observer, i.e.,  $z_2, z_3$  is used. For closed-loop stability analysis, the Lyapunov function  $V$  is defined as  $V = V_c + V_o$ , where  $V_o = \varepsilon^T P \varepsilon$  is the Lyapunov function of the observer and  $V_c \triangleq \frac{1}{2}s^2$  is the Lyapunov function of the controller. The time derivative of  $V_c$  is obtained as

$$\dot{V}_c = s\dot{s} \quad (12)$$

Substituting (11) into (10) leads to

$$\dot{s} = x_3 - z_3 + (\lambda - b/m)(x_2 - z_2) - \frac{kd k_{c1}}{m}s - \frac{kd k_{c2}}{m}\operatorname{sgn}(s) \quad (13)$$

Then, by substituting (13) into (12) we have

$$\dot{V}_c = N\varepsilon s - \frac{kd k_{c1}}{m}s^2 - \frac{kd k_{c2}}{m}\operatorname{sgn}(s)s \quad (14)$$

where  $N = \left[0 - \frac{\lambda - \frac{b}{m}}{\omega_o} - \frac{1}{\omega_o^2}\right]$ . Using (8) and (14) and  $\dot{V} = \dot{V}_c + \dot{V}_o$  we obtain

$$\begin{aligned} \dot{V} &\leq \|N\|\|\varepsilon\|\|s\| - \frac{kd k_{c1}}{m}s^2 - \frac{kd k_{c2}}{m}|s| - \omega_{omin}\|\varepsilon\|^2 \\ &\quad + 2\|PB_1\|\|\varepsilon\|^2 + \frac{2\delta\lambda_{max}(P)\|\varepsilon\|}{\omega_{omin}^2} \end{aligned}$$

Considering the upper bound of  $\varepsilon$ , i.e.,  $\|\varepsilon\| \leq \frac{2\delta\lambda_{max}(P)}{\omega_{omin}^2(\omega_{omin}-2\|PB_1\|)} = \tau$ , after some manipulations we have

$$\dot{V} \leq -\frac{kd k_{c1}}{m}s^2 - \left(-\|N\|\tau + \frac{kd k_{c2}}{m}\right)|s| \quad (15)$$

Now, if  $k_{c2} > \frac{\|N\|\tau m}{kd}$  we assure that  $\dot{V}$  is negative definite. Therefore, by considering the following conditions, the closed-loop stability is guaranteed

- 1) if  $\omega_{omin} > 2\|PB_1\|$ , the estimation errors converge to the bounded balls.
- 2) if  $\omega_{omin} > 2\|PB_1\|$  and  $k_{c2} > \frac{\|N\|\tau m}{kd}$ , both  $s$  and consequently the tracking error converge to zero.

*Remark 1:* The proposed algorithm offers a distinct advantage as it does not require knowledge of the hysteresis model or any information about disturbances. This characteristic makes it particularly appealing for practical applications due to its simplicity and ease of implementation.

*Remark 2:* Ensuring closed-loop stability requires a value of the coefficient  $k_{c2}$  large enough to satisfy  $k_{c2} > \frac{\|N\|\tau m}{kd}$ . On the other hand, since  $k_{c2}$  is the coefficient of the sign term in the control signal, using large values for it can lead to chattering which is undesirable. However, for PEA, due to the small values of  $\frac{m}{kd}$  (it is about  $3.4 \times 10^{-6}$  in the experimental setup), and  $\tau$  (upper bound of the estimation error which is small since the states are small), the lower bound on  $k_{c2}$  is very small. Therefore, a small value for  $k_{c2}$  can be selected to avoid chattering.

#### V. SIMULATION RESULTS

In this section, the performance of the FESO-based control algorithm is assessed through simulation. The simulation is performed using Matlab and Simulink software. The model used for PEA (as the plant under control) is a Bouc-Wen model in (1) whose parameters are identified using data from the experimental setup. Notice that the proposed control structure is model-free, thus the model obtained here is only used for simulating the PEA, not for controller design. The sampling frequency, similar to the experimental tests, is selected as 1 KHz.

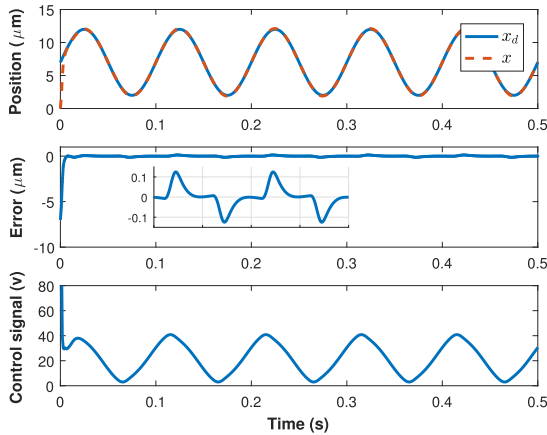


FIGURE 2. Tracking performance of the FESO-SMC algorithm.

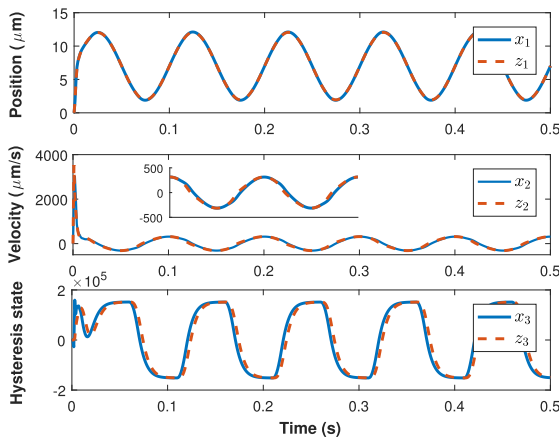


FIGURE 3. Estimation performance of FESO observer.

A sinusoidal reference signal with a frequency of 10 Hz and amplitude of 5 μm is used for the assessment. Fig. 2 depicts the tracking performance of the proposed controller. Furthermore, Fig. 3 illustrates the observer’s ability to estimate the unknown terms and the states of the system. The experimental results were in accordance with the simulation, where the hysteresis effect in the system was taken into consideration.

VI. EXPERIMENTAL RESULTS

The experimental setup comprised a 20 μm piezoelectric actuator and a high-voltage amplifier, with the input range of 0 – 10 V and the output range of 0 – 75 V. Signal conditioning devices provide an analog voltage of 0 – 10 V proportional to the PEA position in the range of 0 – 20 μm. All devices are from the Thorlabs company. For communication between software and hardware, a PCI-1711 data acquisition module from Advantech Inc. was utilized. The controller and observer were implemented in Matlab. The experimental setup is shown in Fig. 4. By applying low-frequency sinusoidal input (to avoid the effect of hysteresis), the parameters of the linear part of the PEA

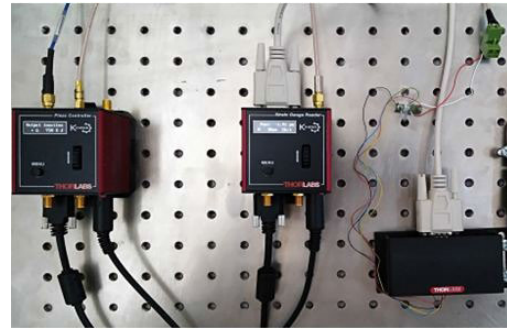


FIGURE 4. Experimental setup.

are obtained, using Matlab’s System Identification toolbox, as  $\frac{b}{m} = 1192$ ,  $\frac{k}{m} = 2.452 \times 10^5$ , and  $\frac{kd}{m} = 2.937 \times 10^5$ .

Various reference trajectories, including sinusoidal and square waves, are considered. For comparison, the performances of four different algorithms, namely the proposed FESO-SMC algorithm, the linear ESO-SMC algorithm, time-delay estimation (TDE)-SMC algorithm, and PI controller, are obtained. To demonstrate the significance of the estimation tool in enhancing controller performance, we employ techniques including FESO, LESO, and TDE. For the TDE algorithm, obtained from [3], the total disturbance is estimated as

$$\hat{D}(t) = D(t - T) = \ddot{x}(t - T) - \frac{b}{m}\dot{x}(t - T) + \frac{k}{m}x(t - T) - \frac{kd}{m}u(t - T)$$

where  $T$  is the sampling time. Then, a robust exact differentiator (RED) [3] is utilized to estimate  $\dot{x}$  and  $\ddot{x}$ . In order to ensure a meaningful comparison, we use the same sliding surface, PD, for FESO-SMC, LESO-SMC, and TDE-SMC. Also,  $\omega_o$  of LESO is selected equal to  $\omega_{omax}$  of FESO. Additionally, the same control gain  $k_{c1,2}$  is used for LESO-SMC and FESO-SMC. The root mean square error (RMSE) and the maximum absolute error (MAE) are then calculated to evaluate the performance of the four controllers. For better verification, MAE is calculated after the transient response. Also, root mean square (RMS) of the control signal is calculated and compared as a measure of control effort.

The experimental results are obtained for three different reference trajectories, as explained in the following.

1) SINUSOIDAL REFERENCE

Let  $x_d = 5 \sin(20\pi t) + 7 \mu\text{m}$ . The experimental results are depicted in Fig. 5. The FESO-SMC controller has a smaller peaking value in comparison to the other three controllers. As observed in Fig. 5, the convergence times of tracking error to a zone around zero for the FESO-SMC, LESO-SMA, TDE-SMC, and PI controllers are approximately 0.031, 0.07, 0.075, and 0.06 s, respectively. RMSE, MAE, and RMS control for the four controllers are reported in Table 1. Furthermore, the FESO-SMC controller shows the smallest initial control effort compared to the other three controllers.

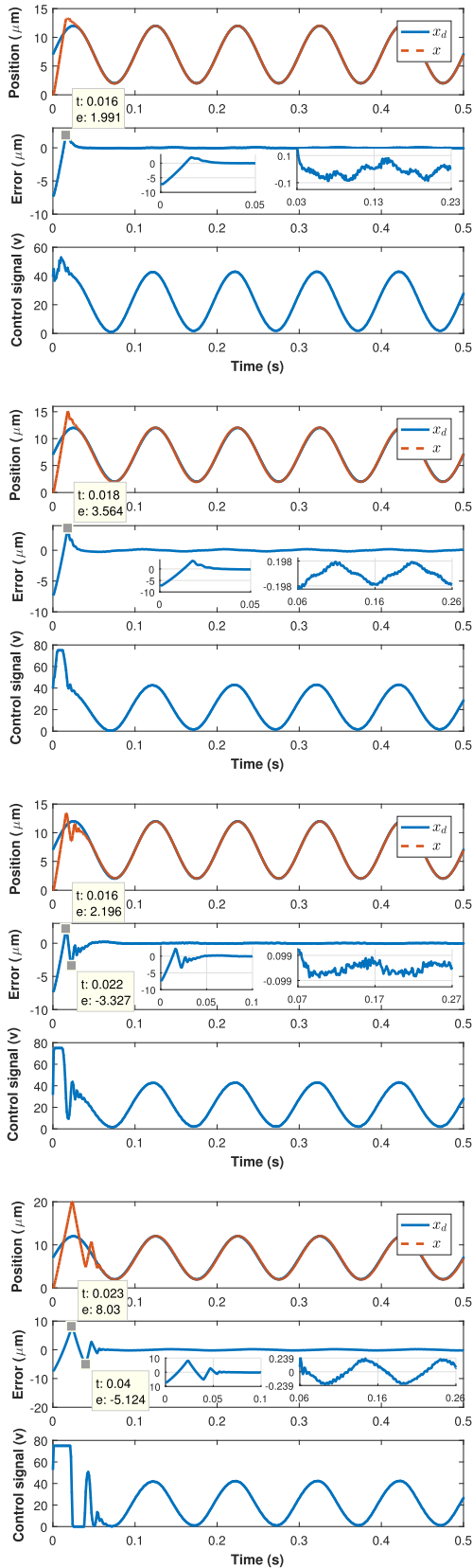


**FIGURE 5.** Tracking performance of the FESO-SMC (top), LESO-SMC (middle1), TDE-SMC (middle2), and PI (bottom) algorithms with  $x_d = 5 \sin(20\pi t) + 7 \mu\text{m}$ .

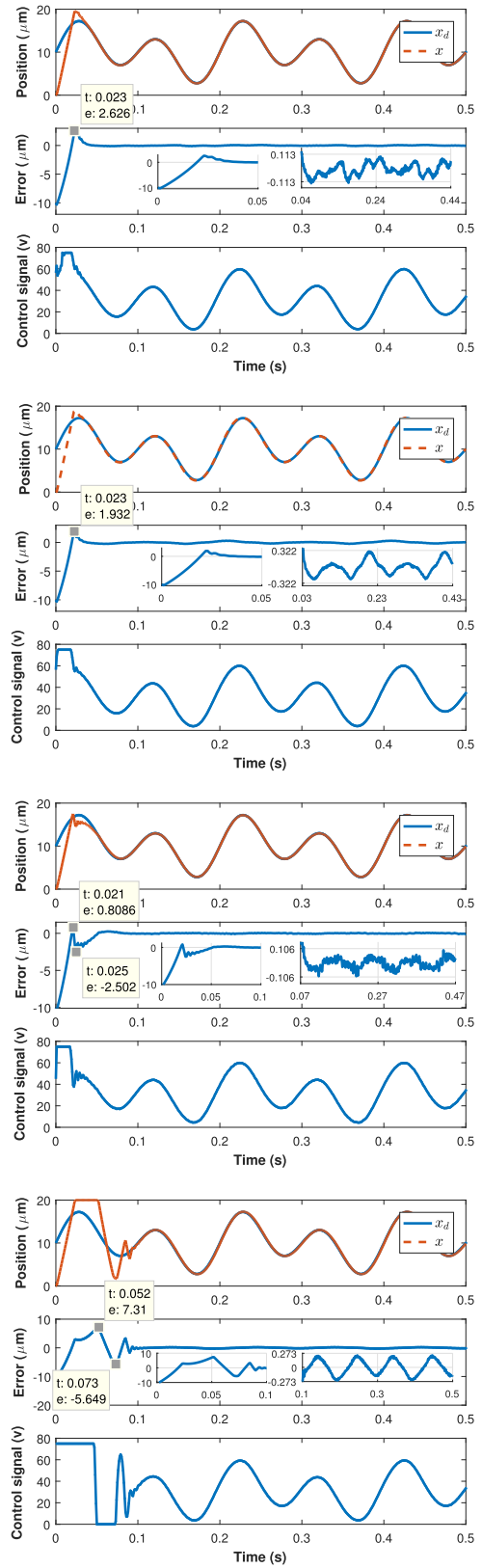


**FIGURE 6.** Tracking performance of the FESO-SMC (top), LESO-SMC (middle1), TDE-SMC (middle2), and PI (bottom) algorithms with  $x_d = 5 \sin(20\pi t) + 3 \sin(10\pi t) + 10 \mu\text{m}$ .

**TABLE 1.** Tracking performance of the four controllers with  $x_d = 5 \sin(20\pi t) + 7 \mu\text{m}$ .

Controller	RMSE	MAE	RMS Control
PI	0.443	0.239 $\mu\text{m}$	26.60 v
TDE-based SMC	0.275	0.099 $\mu\text{m}$	26.87 v
LESO-based SMC	0.288	0.198 $\mu\text{m}$	26.90 v
FESO-based SMC	0.258	0.100 $\mu\text{m}$	26.68 v

2) MULTI-FREQUENCY SINUSOIDAL REFERENCE

Let  $x_d = 5 \sin(20\pi t) + 3 \sin(10\pi t) + 10 \mu\text{m}$ . The experimental results are depicted in Fig. 6, the convergence time of tracking error to a zone around zero for the FESO-SMC, LESO-SMC, TDE-SMC, and PI controllers are about 0.041, 0.033, 0.079, and 0.102 s, respectively. RMSE, MAE, and RMS control for the four controllers are reported in Table 2.

**TABLE 2.** Tracking performance of the four controllers with  $x_d = 5 \sin(20\pi t) + 3 \sin(10\pi t) + 10 \mu\text{m}$ .

Controller	RMSE	MAE	RMS Control
PI	0.647	0.273 $\mu\text{m}$	35.32 v
TDE-based SMC	0.441	0.106 $\mu\text{m}$	35.27 v
LESO-based SMC	0.451	0.322 $\mu\text{m}$	35.42 v
FESO-based SMC	0.440	0.113 $\mu\text{m}$	35.23 v

3) SQUARE WAVE REFERENCE

For the third experiment, first a step reference with an amplitude of 10  $\mu\text{m}$  is considered. The results are depicted in Fig. 7. The RMS error and RMS control for the four controllers are reported in Table 3. It can be observed that, the FESO-SMC, LESO-SMC, TDE-SMC, and PI controllers have almost the same transient response speed, while the overshoot ( $M_p$ ) for FESO-SMC is less than the other three. We can also observe that the PI controller has no proper

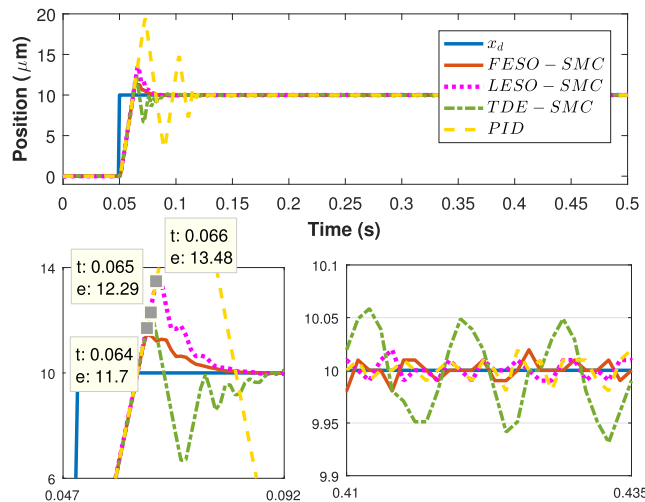


**FIGURE 7.** Tracking performance of FESO-SMC, LESO-SMC, TDE-SMC, and PI algorithms with step reference.

**TABLE 3.** Tracking performance of the four controllers with step reference.

Controller	RMSE	RMS Control	$T_s$	$M_p$
PI	1.722 $\mu\text{m}$	33.82 v	0.064 s	94.4%
TDE-based SMC	1.062 $\mu\text{m}$	34.69 v	0.028 s	22.9%
LESO-based SMC	1.058 $\mu\text{m}$	32.72 v	0.027 s	34.8%
FESO-based SMC	1.019 $\mu\text{m}$	33.63 v	0.023 s	17%

performance for tracking square waves with a frequency of 10 Hz or more.

Next, a square wave reference with the frequency of 10 Hz and amplitude of 4  $\mu\text{m}$  is considered for FESO-SMC, LESO-SMC, and TDE-SMC controllers, as shown in Fig. 8. After the first period, the FESO-SMC obtains a settling time ( $T_s$ ) of 0.01 s without overshoot, while the LESO-SMC has a settling time of 0.023 s with an overshoot around 26% and TDE-SMC has a settling time of 0.023 s with an overshoot of around 24.8%. By comparing the three controllers with different estimation techniques, it can be observed that the fuzzy-based observer, FESO, improves the tracking results.

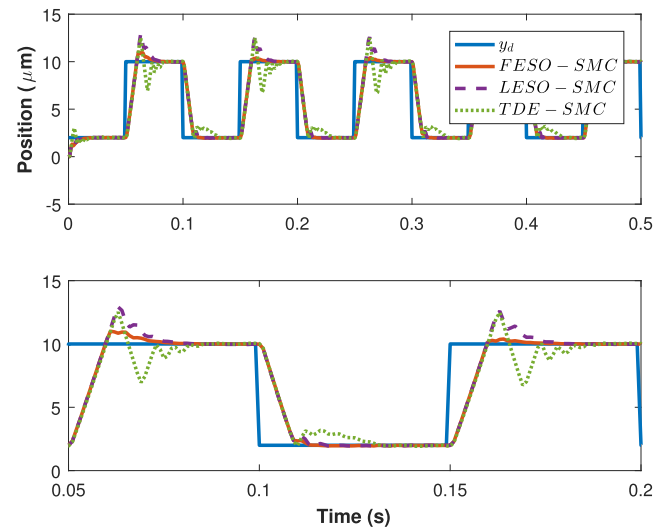


**FIGURE 8.** Tracking performance of FESO-SMC, LESO-SMC, and TDE-SMC for a square wave reference.

VII. CONCLUSION

Due to hysteresis, the precision motion tracking of PEAs has become a challenging task. In this paper, to provide the desired performance of PEAs, a robust observer-based controller constituted by an FESO observer and SMC controller was proposed. Using FESO eliminates the need for identification and inversion of hysteresis to compensate for the hysteresis effect.

To evaluate the tracking performance of the proposed algorithm, the reference trajectories of continuous and discontinuous signals were considered. The transient behavior of PEA was inadequate under the PI, LESO-SMC, and TDE-SMC controllers. The results confirmed the satisfactory performance of the FESO-SMC algorithm in both the

transient and steady-state parts. Furthermore, the stability and tracking of the proposed algorithm were demonstrated using the Lyapunov theory and a joint stability analysis. As part of our future research efforts, we will integrate FESO and TDE methods to enhance the estimation of total disturbance and incorporate it into the control structure of PEA. This approach is expected to yield improvements in the performance of the control system, and we look forward to exploring its potential in detail. Another future research direction is to modify the control structure for higher excitation frequencies. The severe growth of the hysteresis nonlinearity with exciting frequency, as well as structural limitations of PEA, restrict the application of the proposed controller in high excitation frequencies, which will also be addressed in our future research.

## REFERENCES

- [1] M. Al Janaideh, M. Rakotondrabe, I. Al-Darabsah, and O. Aljanaideh, "Internal model-based feedback control design for inversion-free feedforward rate-dependent hysteresis compensation of piezoelectric cantilever actuator," *Control Eng. Pract.*, vol. 72, pp. 29–41, Mar. 2018.
- [2] V. Hassani, T. Tjahjowidodo, and T. N. Do, "A survey on hysteresis modeling, identification and control," *Mech. Syst. Signal Process.*, vol. 49, nos. 1–2, pp. 209–233, Dec. 2014.
- [3] M. Xie, S. Yu, H. Lin, J. Ma, and H. Wu, "Improved sliding mode control with time delay estimation for motion tracking of cell puncture mechanism," *IEEE Trans. Circuits Syst. I, Reg. Papers*, vol. 67, no. 9, pp. 3199–3210, Sep. 2020.
- [4] J. Y. Lau, W. Liang, and K. K. Tan, "Motion control for piezoelectric-actuator-based surgical device using neural network and extended state observer," *IEEE Trans. Ind. Electron.*, vol. 67, no. 1, pp. 402–412, Jan. 2020.
- [5] L. Kong, D. Li, J. Zou, and W. He, "Neural networks based learning control for a piezoelectric nanopositioning system," *IEEE/ASME Trans. Mechatronics*, vol. 25, no. 6, pp. 2904–2914, Dec. 2020.
- [6] D. V. Sabarianand, P. Karthikeyan, and T. Muthuramalingam, "A review on control strategies for compensation of hysteresis and creep on piezoelectric actuators based micro systems," *Mech. Syst. Signal Process.*, vol. 140, Jun. 2020, Art. no. 106634.
- [7] G.-Y. Gu, L.-M. Zhu, C.-Y. Su, H. Ding, and S. Fatikow, "Modeling and control of piezo-actuated nanopositioning stages: A survey," *IEEE Trans. Autom. Sci. Eng.*, vol. 13, no. 1, pp. 313–332, Jan. 2016.
- [8] P.-B. Nguyen, S.-B. Choi, and B.-K. Song, "A new approach to hysteresis modelling for a piezoelectric actuator using Preisach model and recursive method with an application to open-loop position tracking control," *Sens. Actuators A, Phys.*, vol. 270, pp. 136–152, Feb. 2018.
- [9] S. F. Alem, I. Izadi, F. Sheikholeslam, and M. Ekramian, "Piezoelectric actuators with uncertainty: Observer-based hysteresis compensation and joint stability analysis," *IEEE Trans. Control Syst. Technol.*, vol. 28, no. 5, pp. 1997–2004, Sep. 2020.
- [10] I. Ahmad, "Two degree-of-freedom robust digital controller design with bouc-wen hysteresis compensator for piezoelectric positioning stage," *IEEE Access*, vol. 6, pp. 17275–17283, 2018.
- [11] N. N. Son, C. Van Kien, and H. P. H. Anh, "Parameters identification of Bouc–Wen hysteresis model for piezoelectric actuators using hybrid adaptive differential evolution and Jaya algorithm," *Eng. Appl. Artif. Intell.*, vol. 87, Jan. 2020, Art. no. 103317.
- [12] J. Oh and D. S. Bernstein, "Piecewise linear identification for the rate-independent and rate-dependent Duhem hysteresis models," *IEEE Trans. Autom. Control*, vol. 52, no. 3, pp. 576–582, Mar. 2007.
- [13] Y. Liu, S. Xie, D. Du, and N. Qi, "A finite-memory discretization algorithm for the distributed parameter Maxwell-slip model," *IEEE/ASME Trans. Mechatronics*, vol. 25, no. 2, pp. 1138–1142, Apr. 2020.
- [14] H. Jiang, H. Ji, J. Qiu, and Y. Chen, "A modified Prandtl–Ishlinskii model for modeling asymmetric hysteresis of piezoelectric actuators," *IEEE Trans. Ultrason., Ferroelectr., Freq. Control*, vol. 57, no. 5, pp. 1200–1210, May 2010.
- [15] A. A. Davoodi, I. Izadi, and J. Ghaisary, "Design and implementation of a feedforward feedback controller for a piezoelectric actuator," in *Proc. 27th Iranian Conf. Electr. Eng. (ICEE)*, Apr. 2019, pp. 1070–1074.
- [16] D. Huang, D. Min, Y. Jian, and Y. Li, "Current-cycle iterative learning control for high-precision position tracking of piezoelectric actuator system via active disturbance rejection control for hysteresis compensation," *IEEE Trans. Ind. Electron.*, vol. 67, no. 10, pp. 8680–8690, Oct. 2020.
- [17] Q. Xu, "Precision motion control of piezoelectric nanopositioning stage with chattering-free adaptive sliding mode control," *IEEE Trans. Autom. Sci. Eng.*, vol. 14, no. 1, pp. 238–248, Jan. 2017.
- [18] M. Naghdi and I. Izadi, "Sampled-data model-free adaptive control of piezoelectric actuators with input rate constraint using extended state observer," in *Proc. 26th Int. Conf. Syst. Theory, Control Comput. (ICSTCC)*, Oct. 2022, pp. 219–224.
- [19] J. Li and Y. Pi, "Fuzzy time delay algorithms for position control of soft robot actuated by shape memory alloy," *Int. J. Control, Autom. Syst.*, vol. 19, no. 6, pp. 2203–2212, Jun. 2021.
- [20] B. Brahmi, M. Saad, J. T. A. T. Lam, C. O. Luna, P. S. Archambault, and M. H. Rahman, "Adaptive control of a 7-DOF exoskeleton robot with uncertainties on kinematics and dynamics," *Eur. J. Control*, vol. 42, pp. 77–87, Jul. 2018.
- [21] M. Naghdi and M. A. Sadriani, "A novel fuzzy extended state observer," *ISA Trans.*, vol. 102, pp. 1–11, Jul. 2020.
- [22] Z.-L. Zhao and B.-Z. Guo, "Extended state observer for uncertain lower triangular nonlinear systems," *Syst. Control Lett.*, vol. 85, pp. 100–108, Nov. 2015.



**MARYAM NAGHDI** received the M.S. degree in electrical engineering and control from Shahrood University of Technology, Iran, in 2014. She is currently pursuing the Ph.D. degree with the Department of Electrical and Computer Engineering, Isfahan University of Technology, Isfahan, Iran. Her main research interests include fault detection, observer design, sampled-data systems, and piezoelectric actuators.



**IMAN IZADI** received the B.Sc. degree from the Sharif University of Technology, Tehran, Iran, the M.Sc. degree from Isfahan University of Technology, Isfahan, Iran, and the Ph.D. degree from the University of Alberta, Edmonton, Canada, all in electrical engineering. He was a Solutions Specialist with Honeywell Process Solutions, from 2006 to 2012. Then, he joined the Department of Electrical and Computer Engineering, Isfahan University of Technology, where he is currently an Associate Professor.

...